Screening of catalysts for the oxidative dehydrogenation of ethyl lactate to ethyl pyruvate, and optimization of the best catalysts

M. Huchede, D. Morvan, V. Belliere-Baca, J. Millet

Screening of catalysts for the oxidative dehydrogenation of ethyl lactate to ethyl pyruvate, and optimization of the best catalysts.

M. Huchede[1], D. Morvan[2], V. Bellière-Baca[2], J.M.M. Millet[1*]

[1] *Univ Lyon, Université Claude Bernard Lyon 1, CNRS, IRCELYON - UMR 5256, 2 Av. Albert Einstein, 69626 Villeurbanne (France)*

[2] *Adisseo, Antony Parc 2, 10 Place Général de Gaulle, 92160 Antony, France*

`

* Corresponding author: jean-marc.millet@ircelyon.univ-lyon1.fr

1. Introduction

Lactic acid and lactates have been the precursors of choice for the production of industrial chemicals. Indeed, they can be sustainably produced from biomass, by fermentation [1]. One of the most relevant and economically interesting applications for these compounds could be their transformation into other important and valuable compounds, such as pyruvic and acrylic acids, or propanediol [2]. The latter compounds are widely used in the pharmaceutical and cosmetics industry, and in food processing. There is thus renewed interest in the development of efficient catalysts for the oxidative dehydrogenation of lactic acid to pyruvic acid, or for its dehydration to acrylic acid [3-5].

The main difficulty encountered in this type of research is the low selectivity obtained, which is due firstly to the hydrolysis of esters and their further transformation, and secondly to over-oxidation of the reaction product or intermediates. Moreover, both lactic acid and pyruvic acid lack in stability. Lactic acid decomposes easily to acetaldehyde, propanoic acid and CO_x. In addition, it tends to polymerize at high temperatures [6]. Pyruvic acid decomposes also to CO_x and hydroxyethylidene, which isomerizes to acetaldehyde. One of the techniques used to at least partially solve this problem involves dehydrating or oxidatively dehydrogenating the alkyl lactates to the corresponding alkyl acrylates or alkyl pyruvates [7-9]. The resulting esters are more stable from the thermal point of view, and do not form oligomers. Furthermore, as they are more volatile they are easier to spray and do not need to be diluted in water, as in the case of the related acids. This last point is quite important when considering the productivity of an industrial process.

Among the alkyl lactates (methyl, propyl, isopropyl, ...), ethyl lactate is generally preferred, as it is considered to be a commodity chemical and is therefore inexpensive. Indeed, ethyl lactate can be used as a food additive and in the manufacture of fragrances [10]. However, it is used mainly as a solvent, with a particularly attractive application in the coatings industry due to its high solvation power [11]. Although the cost of ethyl lactate currently ranges between $ 0.75 and $ 1.00 per kilogram, a drop in price of up to ~ $ 0.50 per kilogram is projected, which would allow it to compete directly with

petroleum-derived solvents. The ethyl lactate oxidative dehydrogenation reaction can be carried out in the gas or liquid phases. The latter type of reaction leads to processes that make it possible to avoid over-oxidation of the pyruvate, but are less well adapted to production on an industrial scale [12-15]. The reaction requires expensive noble metal catalysts for the activation of oxygen, and in general requires the presence of an excess of a base such as NaOH or LiOH. It is interesting to note the interesting results reported in two very recent studies [16, 17], the first of which describes the apparently efficient use of titanosilicalite (TS-1) in the presence of hydrogen peroxide [16]. Oxidation was carried out in a closed reactor, with one equivalent of H_2O_2 and 20% by weight of TS-1 relative to ethyl lactate. After 5 h at 70 °C in tert-butanol, the ethyl pyruvate yield was 79%. The second and more recent study proposed the use of a mesoporous vanadium titanium mixed oxide catalyst [8]. The liquid-phase aerobic oxidation of ethyl lactate to ethyl pyruvate was carried out with O_2 in diethyl succinate at 130°C. Although a selectivity to ethyl pyruvate greater than 90% was reported, the best yield never exceeded 55% after 5 h of reaction.

Ethyl lactate can be efficiently oxidized in the liquid phase, but from an industrial point of view it is undeniably more advantageous to run the reaction in the gas phase, especially if production units of several hundred thousand tons per year are envisaged. For this reason, the present study focuses on this technology, in particular on the development of the most suitable catalyst for the reaction. Until now, two main types of catalytic system have been studied: mixed oxides or supported transition metal oxides, and silica-supported silver catalysts. If we focus on the most efficient catalysts of the first type, two of them stand out in in the literature: VPO_x/SiO_2 and TeO_2-MoO_3, [17-18]. Although the yield in ethyl pyruvate obtained over these catalysts was always higher than 40%, none are found to be totally satisfactory.

The best patented catalyst is certainly VPO_x/SiO_2 (molar ratio P / V = 10), using air as the oxidant and diluent [17]. The best performance reported with this catalyst was achieved at 200 °C, with conversion around 90% and a selectivity of 60%. However, the reaction was run with an extremely

diluted flux of ethyl lactate gas, which is hardly compatible with an industrial application. Furthermore, catalyst losses phosphorus over time and it is necessary to often add some to the reaction stream.
The TeO_2-MoO_3 catalyst, which main active component was the phase gives 90% selectivity to ethyl pyruvate for 80% of conversion at 300°C [18]. However, deactivation of this catalyst was reported, arising from the reduction of tellurium to metallic tellurium, thus limiting its potential for industrial applications.

The second family consisting of metallic silver, in bulk or supported form, are industrial catalysts of choice for dehydrogenation reactions. They have been used for the production of formaldehyde from methanol, and are very effective for the conversion of allyl alcohol to acrolein, and ethanol to acetaldehyde [19-22]. The use of silica-supported metallic silver for the oxidative dehydrogenation of ethyl lactate has been patented [23]. The best yield, equal to approximately 80%, was obtained on a catalyst having a silver content varying between 20 and 40% by mass, doped with 0.2% Pd. However, it should be noted that the reported catalytic properties were obtained with a gas mixture lying within the explosivity range of ethyl lactate and with a low productivity, thus compromising its application to industrial processes.

Since none of the effective catalysts were found to be suitable for industrial applications, we screened them in an effort to reveal any new, potentially efficient catalyst for the oxidative dehydrogenation of ethyl lactate. Several oxidative dehydrogenation catalysts were thus selected, synthesized and characterized. The choice of catalysts was made on the basis of their oxidation-reduction and acid-base properties, as well as the catalytic characteristics previously demonstrated in oxidative dehydrogenation reactions with similar compounds. This initial screening phase corresponded to the first objective of our study. The best candidate resulting from this selection process was a poly-oxometallate based catalyst. The second aim of the study was then to analyze this compound in greater detail, in an attempt to understand how this catalyst works and optimize its composition.

2. Experimental

2.1. Catalysts synthesis

$FeVO_4$, was synthesized by co-precipitation from an aqueous solution (20 ml) containing 6 mmol of NH_4VO_4 maintained at 50°C under stirring [24]. This solution was added to a similar solution containing 6 mmol of $Fe(NO_3)_3.9H_2O$. The pH was adjusted to 1 with HNO_3 (65%) and the suspension was stirred for 20 min. The pH was then adjusted to 4 by adding NH_3 (32%) and the suspension heated for 2 h at 50°C under stirring. The solid was finally isolated by centrifugation, washed with distilled water (2 × 30 ml), dried for 12 h at 90°C and then calcined for 3 h at 600°C. Iron molybdate, $Fe_2(MoO_4)_3$, was synthesized from an aqueous solution (100 ml) containing 2.2 mmol of $(NH_4)_6Mo_7O_{24}$ and another aqueous solution (50 ml) containing 10.0 mmol of $Fe(NO_3)_3.9H_2O$. The two solutions were mixed and vigorously stirred for 1 h at 25°C. The water was then evaporated under vacuum (10 mbar) at 70°C. The solid formed was dried for 12 h at 90°C and calcined for 3 h at 500°C. Iron and vanadium antimonate, $Fe_{0.4}V_{0.6}SbO_4$, ($FeVSbO_4$) was synthesized from an aqueous solution (150 ml) containing 8 mmol of NH_4VO_3 and 5.3 mmol of $Fe(NO_3)_3.9H_2O$, maintained at 80°C [25]. After complete dissolution, 7 mmol of Sb_2O_3 are added and the resulting suspension is refluxed for 18 h under stirring. The water is then evaporated under vacuum (10 mbar) at 70°C. The solid was dried for 12 h at 90°C and then calcined for 3 h at 200°C. and then for 2 h at 700°C. under air. The mixed oxide Te_2MoO_7 was synthesized by precipitation from an aqueous solution (20 ml) containing 0.3 mmol of $(NH_4)_6Mo_7O_{24}.4H_2O$, to which was added a similar solution containing 4.3 mmol of H_6TeO_6. The solution is then kept at 60°C, with stirring, until a white paste is obtained. The paste was dried for 12 h at 90°C. and then calcined for 2 h at 470°C under air [26].

Molybdenum oxide was synthesized by precipitation from an aqueous solution (10 ml) containing 1 mmol of $(NH_4)_6Mo_7O_{24}.4H_2O$ maintained at 60°C with stirring [27]. A similar solution containing 1 mmol of citric acid was added to the previous solution and the reaction medium was heated for 6 h at

90°C. The precipitate formed was isolated by centrifugation, washed with distilled water (2 × 30 ml), dried for 12 h at 90°C and then calcined for 3 h at 500°C in air.

$FePO_4$ was prepared using a protocol described elsewhere [28]. The ferric salt of phosphomolybdic acid, $FePMo_{12}O_{40}$, was prepared by precipitation [29,30]. An aqueous solution (5 ml) containing 1 mmol of $Fe(NO_3)_3.9H_2O$ was added dropwise to a similar solution containing 1 mmol of $H_3PMo_{12}O_{40}$ (Aldrich ref. 431400). The phosphomolybdic acid being hydrated, its hydration rate was determined by thermogravimetric analysis prior to this operation. It was of 15.3 molecules per Keggin unit (K.U.). The resulting yellow suspension was maintained at 50°C for 1 h. The water was then evaporated under vacuum (10 mbar) at 70°C. The solid obtained was dried for 12 h at 90°C. and calcined for 5 h at 350°C in air. The synthesis of the acids substituted by iron and cesium ($Cs_2Fe_xPMo_{12}O_{40}$ with x=0.0, 0.1, 0.2 and 0.33 and named Cs_2Fe_x) was carried out according to the same protocol using a solution of iron nitrate and cesium nitrate.

The $VTiPO_x$ mixed oxide was prepared by hydrothermal synthesis from an aqueous solution (10 ml) containing 21.2 mmol of $TiCl_4$, the pH of which was adjusted to 8 with NH_3 (32%) [31]. Then, 61.4 mmol of H_3PO_4 (85%) were added to the previous solution. An aqueous solution containing 10.4 mmol of NH_4VO_3 and 20 ml of an equivolumic mixture of lactic acid and distilled water was maintained at 80°C. This solution was added to the titanium solution with stirring. The suspension obtained was then placed in a 30 ml microwave reactor and heated at 175°C for 15 min (700 W, 35°C.min^{-1}). The solid formed was isolated by centrifugation, washed with distilled water (2 × 30 ml) and dried for 12 h at 90°C. The solid $W_{0.75}V_{0.16}Nb_{0.09}O_3$ (MoVNbO) and $MoV_{0.33}O_x$ (MoVO) mixed oxide were also synthesized hydrothermally was according to the synthesis method [32]. To an aqueous solution (40 ml) containing 4.9 mmol of $(NH_4)_6Mo_7O_{24}.4H_2O$ was added a similar solution containing 2.4 mmol of $VOSO_4.xH_2O$. The resulting suspension was stirred under nitrogen for 20 min (20 ml.min^{-1}) to remove dissolved oxygen, and pH was adjusted to 2.6 The mixture was placed in a 100 ml Teflon autoclave and heated for 48 h at 175°C. The resulting solid was then isolated by centrifugation, washed with distilled water (2 × 30 ml), dried for 12 h at 90°C, then calcined for 2 h at 500°C, under nitrogen (100 ml.min^{-1}, 5°C.min^{-1}). The final solid (1g) was suspended in 25 ml of an aqueous solution of oxalic acid (0.4 mol.l^{-}

[1]) and maintained for 30 min at 60°C, with stirring. The solid was isolated by centrifugation, washed with distilled water (2 × 30 ml) and dried for 12 h at 90°C.

The mixed oxide $MoV_{0.30}Nb_{0.17}Te_{0.14}O_x$, (MoVTeNbO) more commonly called M1 phase, was obtained by precipitation [33]. A first aqueous solution containing $(NH_4)_6Mo_7O_{24}.4H_2O$, NH_4VO_3 and H_6TeO_6 was stirred at 80°C until complete dissolution. A second solution containing $Nb_2O_5.xH_2O$ and oxalic acid (molar ratio Nb / oxalate = 3) was heated to 100°C until complete dissolution. The latter was then added to the first solution, resulting in a ratio Mo/V/Te/Nb = 1 / 0.27 / 0.16 / 0.14. After stirring for 30 min at 25°C, the water was then evaporated under vacuum at 80 °C. and the solid is dried for 12 h at 90°C. and then calcined for 4 h at 300°C in air (100 $ml.min^{-1}$, 5°$C.min^{-1}$), then 4 h at 600°C under nitrogen (100 ml.min-1, 5°$C.min^{-1}$). The final solid (1 g) was suspended in 10 ml of a hydrogen peroxide solution (30%) and kept at 60°C for 2 h. The solid was isolated by centrifugation, washed with distilled water (2 × 30 ml) and dried for 12 h at 90°C.

Titanium pyrophosphate $Ti_2P_2O_7$ was prepared from an aqueous solution (70 ml) containing 6 ml of lactic acid (85%), 0.6 ml of ammonia (32%) and 16.7 mmol of $TiCl_4$ [34]. To this solution were added, with stirring, 33.4 mmol of H_3PO_4 (85%). The water was evaporated at 50°C. at atmospheric pressure and the solid calcined for 6 h at 300°C., then 6 h at 450°C. and finally 6 h at 600°C, under air (100 $ml.min^{-1}$, 5°$C.min^{-1}$).

The mixed hydroxyphosphate $Fe_3(PO_4)_2(OH)_2$, was prepared by hydrothermal synthesis. In 20 ml of distilled water were dissolved 2.6 mmol of H_3PO_4 (85%), 1.3 mmol of $FeCl_3$ and 0.67 mmol of $FeC_2O_4.2H_2O$ [35]. The solution was then placed in a 30 ml microwave reactor and heated at 200°C for 10 min. The solid was isolated by centrifugation, washed with distilled water (2 × 30 ml) and then dried for 12 h at 90°C.

The vanadium oxide supported on mesoporous silica, VO_x/SiO_2, at 1% by weight, was prepared by dissolving 0.34 mmol of NH_4VO_3, 1 g of CTAB and 11 g of NH_4Cl in 65 ml of distilled water [36]. The pH of the solution was then adjusted to 5.5 before addition of 31.3 mmol of TEOS. After 24 h at 40°C, the precipitate was isolated by centrifugation, washed with distilled water at 80°C (2 x 30 ml) and then stirred for 2 h under reflux in ethanol. The solid was again isolated by centrifugation, dried for 12 h at 90°C and calcined for 6 h at 650°C in air (100 $ml.min^{-1}$, 5°$C.min^{-1}$). The copper oxide supported on γ-

alumina (20%) CuO/Al_2O_3 was prepared by impregnating 1 g of γ-alumina with 2 ml of an aqueous solution containing 1 mmol of $Cu(NO_3)_2.2.5H_2O$ [37]. The paste formed was left to stand for 1 h at 25°C. under a humid atmosphere, then dried for 24 h at 120°C and calcined for 9 h at 500°C in air (100 $ml.min^{-1}$, 5°C.min^{-1}).

The silver supported on silica Ag/SiO_2 was prepared by impregnation of 5 g of SiO_2 (Cab-O-Sil) with an aqueous solution (10 ml) containing 1.6 mmol of $AgNO_3$ [21]. The paste was then held for 30 min at 25°C, then dried for 24 h at 120°C and calcined for 3 h at 350°C, under air (100 $ml.min^{-1}$.5°C. min^{-1}), then reduced under hydrogen for 5 h at 350°C (5 $ml.min^{-1}$).

Finally, the α and β silicon carbides (α and βSiC) were respectively provided by Sigma Aldrich and the company SICAT. The solids were used without further treatment. Carbon nanotubes (CNT) were provided by Pyrograf Products Inc. (PR-24-XT-PS). Before use, the nanotubes were washed for 2 h in nitric acid (100 $ml.g^{-1}$ CNTs) at reflux. They were isolated by centrifugation and then washed with distilled water until a supernatant of pH = 6 was obtained and dried for 12 h at 120°C.

2.2. Catalysts characterization

The nature and purity of the synthesized phases was checked by X-ray diffraction using a BRUKER D5005 diffractometer with a Ni-filtered CuKα (0.15418 nm) radiation and by atomic absorption (ICP) for chemical analysis. The specific surface areas were measured applying the BET method with nitrogen adsorption. The conventional constant acceleration Mössbauer spectroscope used to characterize iron in the catalysts was home-made [38]. It used a $^{57}Co/Rh$ γ-X-ray source and allowed spectra recording at room temperature. The quantitative analysis of the spectra was made integrating the areas under the individual peaks and assuming equal recoil-free fraction for all species.

2.3. Catalytic testing

The oxidative dehydrogenation of ethyl lactate in ethyl pyruvate has been conducted on all the synthesized compounds in the same conditions using a setup developed in previous studies [39]. In order to develop a competitive industrial process, air was used as oxidizer and the gas stream

composition was above the upper explosive limit of ethyl lactate in the air. It corresponded to a volume ratio of ethyl lactate / O_2 / inert = 12.3 / 18.4 / 69.3. The reaction temperature was varied between 200 and 350°C and the catalyst mass and total gas flow were respectively equal to 250 mg and 65 $ml.min^{-1}$. Any change in these operating conditions will be specifically mentioned. The selectivity and activity data were given after 8 h on stream and stability was evaluated over 22 h.

The condensable reaction products were separated using two traps connected in series, filled with acetonitrile and placed in an ice bath at 0-2°C. The output of the last trap was connected to a μGC-TCD allowing online analysis of gaseous products that cannot be trapped. The μGC was SRA R3000 chromatograph equipped with a molecular sieve, a Porapak Q and a TCD detector. Nitrogen was used as an internal standard. The analysis of the condensed products was carried out on a Shimadzu GC-2014 chromatograph, equipped with a Shimadzu AOC-20i autosampler. The column used was a Nukol type (30 m x 0.53 mm x 0.5 μm) polar capillary column with a flow rate of 3.0 $ml.min^{-1}$ and a split of 50, for an injection of 1 μL. The temperature of the injector and of the FID detector was 220°C. Tetrahydrofuran (THF) was selected as an external standard. The carbon balances for all the catalytic properties evaluated were greater than 98%. Ethyl lactate was not converted between 250 and 350°C in the absence of catalyst.

3. Results and discussion

3.1. Catalyst screening

The twenty prepared catalysts were tested between 200 and 400 °C. By studying the variations in their catalytic properties as a function of reaction temperature, the maximum ethyl pyruvate yields, which can be obtained under the aforementioned experimental conditions, were determined. In general, an increase in reaction temperature leads to an increase in conversion and to a decrease in selectivity to ethyl pyruvate, with a preference for over-oxidation products, thus allowing the maximum yield temperature to be determined.

When designing a catalyst screening test for a given reaction, one of the greatest difficulty encountered is that of selecting the parameters most relevant to the comparison of catalytic performances. Potential parameters include the temperature, gas flow composition, and contact time, under which the catalysts are tested. In order to achieve fair comparisons in the present study, the 20 different catalysts were tested under highly similar operating conditions (flow of reagents, catalyst mass, etc.), which were also chosen in view of their potential industrialization. For each catalyst, the reaction temperature was varied, since it is known that from one catalytic system to another, selectivity to ethyl pyruvate can increase, decrease, or pass through a maximum, as a function of temperature. For this reason, the temperature range over which the best yield is achieved varies for each different catalyst.

Two criteria were chosen for the evaluation of each catalytic system's properties: maximum selectivity to ethyl pyruvate, and maximum yield. The highest selectivity obtained with a catalyst is an important parameter, especially in the case of a process including one or more recycling sequences. Maximum yield and productivity are also very useful parameters for the assessment of a catalyst's efficiency, and its potential use in an industrial process. The results of the screening evaluation are thus presented in the form of two separate figures, which for each catalyst (over the studied temperature range) show in the first one the highest achievable selectivity, as a function of the conversion rate at which this selectivity occurs and in the second, the catalyst's selectivity as a function of the conversion rate at which the maximum yield occurs. The temperature at which each of the maximum values of selectivity was obtained is noted in the first figure, close to the corresponding data point, and the reaction temperature, the maximum yield and the productivity expressed in $mol.s^{-1}.g^{-1}$, are indicated in the second figure. Finally, in order to improve the presentation of these results, the catalysts are grouped into two distinct families, according to whether or not they contain V and Mo. The results obtained for the families of catalysts that contain and do not contain V or Mo are respectively presented in Fig. 1 and 2. All the catalysts tested in this study appear to be active and selective for the reaction of interest, and in all cases ethyl pyruvate was the main product. The main by-products were systematically acetaldehyde, CO_2, ethylene and ethanol. In certain cases, small amounts of acetic acid were detected. A reaction scheme, with reaction paths for each of these by-products, is proposed in Fig. 3.

In this reaction scheme, the main secondary reaction is the hydrolysis of esters to acids and ethanol, which takes place mainly on strong acidic sites. The resulting lactic and pyruvic acids then break down into CO_2 and ethanol or acetaldehyde. Very small amounts of lactic acid and pyruvic acid were detected, but not quantified. The ethanol produced in this reaction can be dehydrated to ethylene on acid sites, or oxidized to acetaldehyde. The acetaldehyde can be oxidized to acetic acid.

The results obtained with V or Mo-containing catalysts show that the highest selectivity to ethyl pyruvate was obtained with $FePMo_{12}O_{40}$ and $FeVSbO_4$ catalysts with 94% and 90%, with respectively 40% and 37% conversion at 250 °C and 300 °C (Fig. 1a). The best yields were obtained on MoO_3 at 300°C with 63% and on the two former catalysts with respectively 57 and 56% at 275 and 300°C (Fig. 1b). On catalysts containing no V or Mo, lower selectivities and maximum yields were systematically observed. Although a selectivity of 84% for ethyl pyruvate was observed at 295 °C on silver supported on silica, the maximum yield with this catalyst was much lower than that observed with the best catalysts from the first series. This type of silver catalyst was also found to be less efficient than what has previously been reported in the literature [23]. The reaction conditions used in the latter study, although certainly more appropriate for this type of catalyst and reaction, would not be suitable for an industrial application, and were different to those used in the present study.

The studied catalysts were stable on stream for about 22 h, with the exception of $Te_2Mo_2O_7$ and MoO_3. In the first case, deactivation has already been reported for the same reaction, and attributed to the reduction and volatilization of Te under the reaction flow, even in the presence of oxygen [18]. In the second case, it is thought that Mo was lost through the gas volatilization of molybdenum oxy-hydroxides species formed at high temperatures in the presence of water. Indeed, Mo was observed at the cold spot at the end of the reactor, when it was run for a long time at high temperatures.

With a selectivity of 95% at 30% conversion, together with a productivity similar to that observed with other catalysts described in the literature, $FePMo_{12}O_{40}$ appears to be the most selective of the twenty catalysts examined in this study. The remainder of this study is thus devoted to a more detailed analysis of its catalytic properties and to their improvement. Furthermore, this type of polyoxometalate is well suited to the use of a wide variety of different compositions obtained by

changing the nature of the counter-cations while keeping the same primary structure and its catalytic properties could potentially be improved by such modification.

3.2. Optimization of phosphomolybdic polyoxometalate catalysts

Although the highest selectivity to ethyl pyruvate was observed with $FePMo_{12}O_{40}$, and this could hardly be improved, its activity over the optimal temperature range needs to be improved. $FePMo_{12}O_{40}$ has a low specific surface area, which is certainly responsible for this low activity and all attempts to improve it by changing the synthesis conditions, have failed. However, a high, stable specific surface area can be achieved with polyoxometalates, by synthesizing them in the form of an alkaline salt [40]. The effect was the most important in the case of cesium salt since it exhibited the highest specific surface area [41,42]. For this reason, a series of phosphomolybdic polyoxometalate catalysts was prepared, using both cesium and iron as counter-cations: two Cs cations per Keggin unit were used, with variable amounts of iron introduced as counter-cations.

XRD characterization of the catalysts showed that, in contrast to $FePMo_{12}O_{40}$, which crystallizes as a mixture of phosphomolybdic acids hydrated with either 13 or 30 water molecules (ICSD 028-0082 and 015-4751), the compounds containing cesium only have the same cubic structure as polyoxometalate salts (ICSD 014-3585) (Fig. 4). The chemical analysis and results of the specific surface area measurements of the catalysts are presented in Table 1. Our chemical analyses showed that their bulk compositions are closely matched to their nominal compositions. The $FePMO_{12}O_{40}$ catalyst used corresponds to a heteropolyacid, in which all of the protons have been substituted by iron. This is possible, thanks to the very high flexibility of the secondary structure of this acid. This type of compound has a low specific surface area (in the present case 2 $m^2.g^{-1}$), which is detrimental to a high level of catalytic activity (Table 1).

Table 1: Results of specific surface area (SSA) measurements, cell parameter calculations, thermo-gravimetric analyses (number of water molecules lost per Keggin unit) and chemical analyses (atomic ratios) of the synthesized samples.

Catalyst	SSA[a] ($m^2.g^{-1}$)	Cell parameter (Å)	H_2O/K.U.			
				Cs/P	Fe/P	Mo/P
$FePMo_{12}O_{40}$	2	-	13.4	-	1.0	11.5
$Cs_2Fe_{0.33}$	35	11.818(3)	-	2.1	0.33	10.4
$Cs_2Fe_{0.2}$	33	11.818(3)	-	2.1	0.21	10.5
$Cs_2Fe_{0.1}$	15	11.817(3)	1.8 (5.5)	2.0	0.10	10.3
Cs_2	9	11.814(3)	3.5 (10.5)	2.2	-	11.8

[a]: specific surface areas were measured after 8 h catalytic testing.

As could be expected, the presence of cesium in the polyoxometalate has a considerable influence on the specific surface area, with values up to 35 $m^2.g^{-1}$ being reached. DTG analyses of the $FePMo_{12}O_{40}$ and $Cs_2Fe_{0.1}$ catalysts showed that the solid containing Cs was considerably less hydrated than that with no Cs. In the latter, despite the presence of iron cations, water molecules were observed at a concentration almost as high as that of the pure acid (15.2 H_2O per K.U.). All the infrared spectra showed only the bands corresponding to the vibrations μ_{as} P-O (around 1060 cm^{-1}), μ_{as} Mo = O (around 968 and 958 cm^{-1}) and μ_{as} Mo-O-Mo (around 859 cm^{-1}), characteristics of heteropolyphosphomolybdic compounds with Keggin-type anions (Fig. S1).

The results of the catalytic testing of the Cs-containing catalysts are compared with those obtained with $FePMo_{12}O_{40}$ in Table 2. The catalysts containing cesium appeared to be active and selective. Although none of them reached the record selectivity of $FePMo_{12}O_{40}$, some of them had higher ethyl pyruvate yields: as an example, a yield of 66 % was obtained on $Cs_2Fe_{0.1}$ at 250°C. The catalysts were very stable with time on stream, at least over a period of 22 h as illustrated for $Cs_2Fe_{0.1}$ in Fig. S2. In the case of the cesium-containing series, the addition of iron was found to have a positive effect on selectivity, with a maximum reached on $Cs_2Fe_{0.2}$, whereas the intrinsic rate of ethyl lactate conversion decreased monotonically with iron content (Fig 5).

Table 2: Catalytic performance of polyoxometalates as a function of reaction temperature under standard testing conditions - EtPa: ethyl pyruvate, ACHO: acetaldehyde, Ethyl: ethylene, Ethol: ethanol, AcA: acetic acid.

Compound	Temp. (°C)	Conv. (%)	Selectivity (%)							EtPa Yield (%)
			EtPa	ACHO	CO_2	Ethyl	Ethol	AcA	Others	
$FePMo_{12}O_{40}$	225	13.4	96.7	1.0	1.0	0.5	0.5	0.0	0.3	12.9
	250	40.3	93.7	1.6	1.7	1.1	1.5	0.0	0.4	37.8
	275	61.2	90.8	2.1	1.6	1.3	1.9	1.0	1.3	55.6
$Cs_2Fe_{0.33}$	200	13 .7	95.0	0.1	1 .2	1.1	0.3	0.0	2.3	
13.0	225	31.4	88.9	1.9	2.7	2.7	1.8	0.0	2.0	27.9
	250	45.3	87.3	2.8	2.9	3.1	1.9	0.0	2.0.	39.5
	275	71.0	82.9	3.7	3.4	3.0	2.5	1.3	3.2	58.9
$Cs_2Fe_{0.2}$	200	13.7	95.0	1.0	1.1	0.5	0.3	0.0	2.1	13.1
	225	40.0	90.4	1.6	2.2	2.2	1.3	0.0	2.1	
36.2	250	62.1	87.2	2.4	2.5	2.8	1.8	1.0	2.3	54.2
	275	76.9	79.3.	3.4	4.1	5.2	2.2	2.1	3.7	61.0
$Cs_2Fe_{0.1}$	200	30.9	94.0	1.1	1.2	1.0	1.1	0.0	1.6	29.0
	225	54.3	89.8	1.7	2.5	2.9	1.5	0.4	1.2	48.8
	250	87.1	76.9	3.1	4.8	8.3	1.9	2.3	2.7	66.9
	275	93.5	62.5	4.7	8.6	13.2	3.5	3.6	3.9	58.4
Cs_2	185	47.0	90.0	2.1	2.4	3.2	0.1	0.2	1.9	42.3
	200	67.4	85.8	2.4	3.6	4.4	1.8	1.4	1.6	57.8
	225	82.2	69.9	4.3	6.2	11.0	1.7	3.1	3.9	57.5

This result is in agreement with the findings of other studies, showing that when iron is present in the counter-cation position, it leads to a decrease in the rates of reduction and re-oxidation of similar solids, and that this effect is improved when the iron content is increased [29]. All the iron-containing catalysts were stable over the studied temperature range, and the structure of the material was maintained after the reaction. This was not the case for the Cs_2 compound, which was unstable at high temperatures and could not be compared to the other compounds under these conditions.

In order to understand the differences in catalytic properties observed with these compounds, in particular $FePMo_{12}O_{40}$ and $Cs_2Fe_{0.33}$, the degree of oxidation and the environment of iron were analyzed by Mössbauer spectroscopy, prior to and following catalytic testing. It was not possible to perform similar analyses on the other substituted compounds, as their iron content was very low. The

isomeric (δ) and quadrupole moment (Δ) displacement values computed from the spectra are listed in Table 3, and their spectra are shown in Fig. 6. The Mössbauer spectra of the $Cs_2Fe_{0.33}$ compound before and after the catalytic test were adjusted with a single doublet with approximately the same hyperfine parameters characteristic of Fe^{3+} ions.

Table 3: Mössbauer parameters calculated from the spectra of the $FePMo_{12}O_{40}$ and $Cs_2Fe_{0.2}$ samples, recorded at 25 °C.

Compound		**Site**	**δ (mm.s^{-1})**	**Δ (mm.s^{-1})**	**%**
$FePMo_{12}O_{40}$	Before test	Fe^{3+}	0.35	0.60	100
	After test	Fe^{3+}	0.30	0.68	60
		Fe^{2+}	1.24	2.47	40
$Cs_2Fe_{0.33}$	Before test	Fe^{3+}	0.24	0.25	100
	After test	Fe^{3+}	0.22	0.31	100

On the other hand, prior to the test, the spectrum of the $FePMo_{12}O_{40}$ was fitted to a ferric doublet, whereas that of the solid after testing was fitted to two doublets - one ferric and the other ferrous. The hyperfine parameters of the ferric doublets computed from the spectra were characteristic of Fe^{3+} in an octahedral coordination [38], whereas the ferrous doublet was characterized by a large quadrupole splitting, typical of a highly distorted environment. The Mössbauer spectra of the $Cs_2Fe_{0.33}$ compound, before and after the catalytic test, were fitted to a single doublet with approximately the same hyperfine parameters characteristic of Fe^{3+} ions and comparable to those reported in the literature for iron counter-cations in polyoxometalates [29].

3.3. Discussion

Although most of the catalysts tested during the screening phase of our study are known to be efficient for oxidative dehydrogenation, their performances vary a lot in terms of activity and selectivity. In the case of the best catalysts obtained from the screening ($FePMO_{12}O_{40}$, $FeVSbO_4$ and MoO_3), in addition to the Ag/SiO_2 catalyst proposed in the literature, there does not appear to be any obvious, common feature explaining their catalytic properties. Although in all cases the latter properties

contribute to oxidative reactions by means of a Mars and van Krevelen mechanism, they involve distinct redox couples: Mo^{6+}/Mo^{5+}, V^{5+}/V^{4+} and Ag^{+}/Ag^{0}, respectively, as well as different bulk constituents and structures. This could lead to the conclusion that the reaction is relatively easy to catalyse, and that different catalysts can be active in the reaction. The best catalysts would be those which are the most active just below the temperature of decomposition of ethyl lactate or pyruvate, i.e. around 330 °C, which is the case for the best catalysts described in this study. Their observed differences in productivity could then be related simply to differences in active surface site densities, or intrinsic surface site activities. In addition, all of the best catalysts have a low surface acidity. This feature was found to be essential, in order to avoid the hydrolysis of esters through the formation of lactic and pyruvic acids, and their subsequent oxidation to lighter by-products. MoO_3 is known to have only weak acid sites [43]. $FePMO_{12}O_{40}$ is an heteropolyacid, in which the protons have been completely replaced by iron cations, thus suppressing all strong acidity, whereas the $FeVSbO_4$ catalyst with the chosen Fe/V ratio (0.66) has been shown to have only very weak acid sites [25]. Ag/SiO_2 has also been shown to be weakly acidic [44,23]. Conversely, WVNbO and TiP_2O_7, which are the least selective among the active catalysts in our selection, are also the most acidic [45,46].

Our efforts to improve the characteristics of the best catalyst, i.e. $FePMO_{12}O_{40}$, were successful in so far as the ethyl pyruvate yield was increased to 67%. This was achieved by adding cesium counter-cations. Alkali metals can also be used to substitute protons, and in the present study were found to precipitate, forming phases with a cubic salt structure and very fine particles (ranging from 10 to 40 nm in diameter). When the protons are not completely substituted by alkali metals, the prepared solids correspond to the hydrated acid together with the pure salt, with the acid phase coating the salt particles [40]. Although the acid cannot be detected by X-ray diffraction, it can be observed by XPS or Raman spectroscopy [40, 47]. When it is added at the same time as the monovalent cation substitute, the iron has been shown to replace the protons in the supported acid [40]. Although in both cases, at a macroscopic level, the transition metals do not appear to have a significant influence on the structural characteristics of the acid, other than decreasing its degree of hydration, they have a strong influence on the catalytic properties of the solids in the oxidation and oxidative dehydrogenation reactions. In the polyoxometalate series studied here, the protons are progressively substituted by iron

cations in the supported acid to $Cs_2Fe_{0.33}$, which should not contain any more protons. This evolution explains the observed increase in the catalyst's selectivity as a function of increasing iron content, although it did not reach the level of the unsupported acid as it should.

In $FePMo_{12}O_{40}$ the iron is present mainly in the form of an octahedral complex hexahydrate $Fe(H_2O)_6^{3+}$, located between Keggin units. Alternatively, if a water molecule is lost, it adopts the form of a $Fe(H_2O)_5^{3+}$ complex bound by terminal oxygen to a heteropolyanion (Fig. 7a) [29, 47]. In this case, DFT calculations have shown that electron transfers between iron and molybdenum can take place: $Mo^{5+} + Fe^{3+} \rightleftharpoons Mo^{6+} + Fe^{2+}$ [48]. This is the reason for which the iron is partially reduced after catalytic testing. This electron transfer has a noticeable influence on the redox activity of Mo, since the intrinsic activity of $FePMo_{12}O_{40}$ is much higher than that of the iron substituted acid supported on cesium salt. In the latter compounds, it has been shown that the iron had a different environment and was present in the form of $(FeOH)^{2+}$ or $(FeOH_2)^{+}$ species (Fig. 7b) [48-50]. This difference may be related to changes brought about by the presence of cesium salt in the structure of the supported acid phase, leading to a strong decrease in the space between the Kegging units. This assumption is supported by the results of the DTG analysis, which show that the hydration water content per Keggin unit of acid is much lower for the supported acid than for the bulk acid. In this case there are no electron transfers, as confirmed by the results of Mössbauer spectroscopy. However, it is important to note that the protons remain, even in the $Cs_2Fe_{0.33}$ compound, thus leading to a higher acidity than in $FePMo_{12}O_{40}$. The acidity of the Cs_2Fe_x compounds has previously been studied using the dehydration of isopropanol to propene as model reaction [29] (Fig. S3). The rate of propene formation and thus the acidity of the compounds decreased when iron content increased up to $Cs_2Fe_{0.2}$. At higher iron content, the loss of protons substituted by iron was compensated by hydroxyl groups bound to iron and the acidity did not decreased anymore [29]. In this respect, the best selectivity to ethyl pyruvate was obtained with $Cs_2Fe_{0.2}$, which confirmed that the less acidic catalysts were well the most selective. It is highly likely that similar phenomena would be observed with transition metal cations other than iron, which does not allow to wait any progress with other substitutions.

4. Conclusion

The screening of various catalysts for the oxidative dehydrogenation of ethyl lactate has led to the identification of several candidates, which could be sufficiently efficient for use in industrial application, especially if an easy separation and recycling of unconverted ethyl lactate is possible.

Among these catalysts, iron-substituted phospho-molybdic heteropoly acid $FePMo_{12}O_{40}$ appears to be the candidate having the highest efficiency. The performance of this catalyst was optimized by means of iron and cesium co-substitution, leading to higher ethyl pyruvate yields under similar reaction conditions. These catalysts, which correspond to iron-substituted acids supported on cesium salt, are substantially more active. This characteristic is related to their significantly higher specific surface area, since the intrinsic activity of their active sites is lower and the selectivity is decreased. The higher intrinsic activity of active sites of $FePMo_{12}O_{40}$ is likely related to an electron transfer between iron and molybdenum that is not present for iron-substituted acid supported on cesium salt. Considering the selectivity, it has been observed that it depends highly on the acidity of the catalysts since the later promotes side-reactions like hydrolysis that decreases the selectivity to ethyl pyruvate. Consequently, the best catalysts appear the ones with numerous redox Mo sites and relatively low acidity i.e. $Cs_2Fe_{0.1}$. The compounds $Cs_2Fe_{0.2}$ and $Cs_2Fe_{0.33}$ are less efficient despite a higher specific surface area and number of active sites and a higher selectivity to ethyl pyruvate. This is due to a lower intrinsic activity of the active sites. Finally, $FePMo_{12}O_{40}$ appears as the most selective catalyst because of its lowest acidity related to its lowest number of protons.

In addition to its concrete application for the design of an efficient catalyst for the oxidative dehydrogenation of ethyl lactate, this study provides an example of the importance of the influence of surface acidity in oxidative dehydrogenation catalysts, and shows how this acidity can vary according to the nature of the counter-cations used in polyoxometalate-based catalysts.

5. Acknowledgment

The authors gratefully acknowledge the ADISSEO company for the financial support it provided for the present study.

6. References

[1] Y. Fan, C. Zhou, X. Zhu, Catal. Rev. 51 (2009) 293-324.

[2] M. Dusselier, P. Van Wouwe, A. Dewaele, E. Makshina, B.F. Sels, Energy Environ. Sci. 6 (2013) 1415-1442.

[3] T. Bonnotte, S. Paul, M. Araque, R. Wojcieszak, F. Dumeignil, B. Katryniok, ChemBioEng Rev. 5 (2018) 34-56.

[4] P. Maki-Arvela, I.L. Simakova, T. Salmi, D. Yu. Murzin, Chem. Rev. 114 (2014) 1909-1971.

[5] E. Blanco, P. Delichere, J.M.M. Millet, S. Loridant, Catal. Today 226 (2014) 185-191.

[6] D.T. Vu, A.K. Kolah, N.S. Asthana, L. Peereboom, C. T. Lira, D. J. Miller, Fluid Phase Equilibria 236 (2005) 125-128.

[7] B.M. Murphy, M.P. Letterio, B. Xu, ACS Catal. 6 (2016) 5117-5131.

[8] W. Zhang, G. Innocenti, P. Oulego, V. Gitis, H. Wu, B. Ensing, F. Cavani, G. Rothenberg, N.R. Shiju, ACS Catal. 8 (2018) 2365-2374.

[9] E. Blanco, C. Lorentz, P. Delichere, L. Burel, M. Vrinat, J.M.M. Millet, S. Loridant, Appl. Catal. B: Env. 180 (2016) 596-606.

[10] Industrial Solvents Handbook" by E.W. Flick. 5th Edition. William Andrew Inc., 1998. ISBN 0-8155-1413-1, ISBN 978-0-8155-1413-8

[11] S.P.J. Ahmadkalaei, S. Gan, H.K. Ng, S.A. Talib, Environ. Sci. Pollut. Res. 23 (2016) 22008-22018.

[12] T. Mallat, A. Baiker, Chem. Rev. 104 (2004) 3037-3058.

[13] T. Tsujino, S. Ohigashi, S. Sugiyama, K. Kawashiro, H. Hayashi, J. Mol. Catal. 71 (1992) 25-35.

[14] S. Sugiyama, T. Kikumoto, H. Tanaka, K. Nakagawa, K.I. Sotowa, K. Maehara, Y. Himeno, W. Ninomiya, Catal. Lett. 13 (2009) 1129-1134.

[15] C. Zhang, T. Wang, Y. Ding, J. Appl. Catal. A: Gen. 533 (2017) 59-65.

[16] S.I. Fang, C.F. Hsieh, C.C. Shih, China Petrochemical Corp., US20140031581, 2014.

[17] F. Thalhammer, K.-H. Schrank, K. Wernthaler, Sueddeutsche Kalkstickstoff, DE19756584, 1999.

[18] H. Hayashi, S. Sugiyama, N. Masaoka, N. Shigemoto, Catal. Lett. 19 (1993) 273-277.

[19] S. Lomate, T. Bonnotte, S. Paul, F. Dumeignil, B. Katryniok. Sustain. Chem. Proc. 3 (2015) 1-8.

[20] M. Qian, M.A. Liauw, G. Emig, Appl. Catal. A : Gen. 238 (2003) 211-222.

[21] T.T.N. Nguyen, M. Huchede, E. Blanco, F. Morfin, J.L. Rousset, L. Massin, M. Aouine, V. Bellière-Baca, J.M.M. Millet, Appl. Catal. A: Gen. 549 (2018) 170-178.

[22] G.J. Millar and M. Collins, Ind. Eng. Chem. Res. 56 (2017) 9247-9265.

[23] J. Shen, W. Ji, Y. Han, Y. Chen, Nanjing University CN1359893, 2002.

[24] L.E. Briand, J.M. Jehng, L. Cornaglia, A.M. Hirt, I.E. Wachs, Catal. Today, 78 (2003) 257-268.

[25] H. Roussel, B. Mehlomakulu, F. Belhadj, J.M.M. Millet, J. Catal. 205 (2002) 97-106.

[26] H. Hayashi, S. Sugiyama, N. Masaoka, N. Shigemoto, Ind. Eng. Chem. Res. 34 (1995)135-139.

[27] K. Chen, S. Xie, A.T. Bell, E. Iglesia, J. Catal. 198 (2001) 232-242.

[28] J.M.M. Millet, J.C. Védrine, Appl. Catal. 76 (1991) 209-219.

[29] M. Langpape, J.M.M. Millet, U.S. Ozkan, P. Delichère, J. Catal. 182 (1999) 148-155.

[30] O. Benlounes, S. Cheknoun, S. Mansouri, C. Rabia, S. Hocine, J. Taiwan, Inst. Chem. Eng. 42 (2011) 132-137.

[31] D. Nagaki, H. Weiner, J.T. Chapman, M.O. Scates, A.S. Locke, C.J. Peterson, Celanese International Corporation, US20120277466, 2012.

[32] A. Chieregato, F. Basile, P. Concepción, S. Guidetti, G. Liosi, M.D. Soriano, C. Trevisanut, F. Cavani, J.M. López Nieto, Catal. Today, 197 (2012) 58-65.

[33] B. Deniau, G. Bergeret, B. Jouguet, J.L. Dubois, J.M.M. Millet, Top. Catal. 50 (2008) 33-42.

[34] I.-C. Marcu, I. Sandulescu, J.M.M. Millet, J. Mol. Catal. A: Chem. 203 (2003) 241-250.

[35] D. Rouzies, J.M.M. Millet, D. Siew Hew Sam, J.C. Vedrine, Appl. Catal. 124 (1995) 189-203.

[36] L.D. Nguyen, S. Loridant, H. Launay, A. Pigamo, J.L. Dubois, J.M.M. Millet, J. Catal. 237 (2006) 38-48.

[37] A.E. Marcinkowsky, J.P. Henry, Union Carbide Corporation, US4220803, 1980**.**

[38] J.M.M. Millet, C. Virely, M. Forissier, P. Bussière, J.C. Vedrine, Hyperfine Interact. 46 (1989) 619-628.

[39] P. Lauriol-Garbey, S. Loridant, V. Bellière-Baca, P. Rey, J.M.M. Millet, Catal. Comm. 16 (2011) 170-174.

[40] M. Langpape, J.M.M. Millet, U.S. Ozkan and M. Boudeulle, J. Catal. 181, (1999) 80-90.

[41] M. Mizuno, M. Misono, Chem. Rev. 98 (1998) 199-218.

[42] S. Paul, W. Chu, M. Sultan and E. Bordes-Richard, Sci. Chin. Chem. 53 (2010) 2039-2046.

[43] K. Routray, W. Zhou, C.J. Kiely, W. Grünert, I.E. Wachs, J. Catal. 275 (2010) 84-98.

[44] W. Janssens, E.V. Makshina, P.Vanelderen, F. De Clippel, K. Houthoofd, S. Kerkhofs, J.A. Martens, P.A. Jacobs and B.F. Sels, ChemSusChem 8 (2015) 994-1008.

[45] A. Chieregato, M.D. Soriano, F. Basile, G. Liosi, S. Zamora, P. Concepción, F. Cavani, J.M. López Nieto, Appl. Catal. B: Env. 150-151 (2014) 37-46.

[46] I.-C. Marcu, I. Sãndulescu, Ana. Univ. Bucureúti, Chimie, Anul XII (serie nouă), vol. I-II, pag. 309-313.

[47] Staroverova I.N., Kutyrev M., Stakheev A., Kinetika i Kataliz 33 (1) (1992) 127-133.

[48] S.A. Borshch, H. Duclusaud, J.M.M. Millet, Appl. Catal. A: Gen. 200 (2000) 103-108.

[49] E. Etienne, F. Cavani, R. Mezzogori, F. Trifirò, G. Calestani, L. Gengembre, M. Guelton, Appl. Catal. A: Gen. 256 (2003) 275-290.

[50] Q. Huynh, J.M.M. Millet, J. Phys. and Chem. Solids 66 (2005) 887-894.

FIGURES CAPTION

Figure 1: Catalytic properties of catalysts containing V and Mo: (a) best selectivity to ethyl pyruvate as a function of ethyl lactate conversion, showing the reaction temperature (°C) at which it was obtained, (b) selectivity to ethyl pyruvate as a function of ethyl lactate conversion at best yield, showing the reaction temperature (°C) at which it was obtained, together with the corresponding yield in %.

Figure 2: Catalytic properties of catalysts that do not contain V or Mo: (a) best selectivity to ethyl pyruvate as a function of ethyl lactate conversion, showing the reaction temperature (°C) at which it was obtained, (b) selectivity to ethyl pyruvate as a function of ethyl lactate conversion at best yield, showing the reaction temperature (°C) at which it was obtained, together with the corresponding yield in %.

Figure 3: Reaction scheme for the formation of quantized by-products in the oxidative dehydrogenation of ethyl lactate to ethyl pyruvate for all tested catalytic systems.

Figure 4 : X-ray diffraction patterns of the prepared phosphomolybdic polyoxometalates : a) $FePMo_{12}O_{40}$, b) $Cs_2Fe_{0.3}$**,** c) $Cs_2Fe_{0.3}$ and d) $Cs_2Fe_{0.33}$.

Figure 5: a) Rate of ethyl lactate conversion and selectivity to ethyl pyruvate b) selectivity to by-products as a function of the iron content of the catalysts. ethanol (△), ethylene (■), CO_2 (▲), acetaldehyde (◆), acetic acid (▽) and others (❍). Catalytic reaction conditions: ethyl lactate / O_2 / inert = 12.3 / 18.4 / 69.3 and temperature =225 °C.

Figure 6: Mössbauer spectra of two compounds: $Cs_2Fe_{0.33}$ a) and b) and $FePMo_{12}O_{40}$ c) and d), recorded at 25 °C before and after catalytic testing; solid lines are derived from least-squares fits.

Figure 7: Model clusters representing the interaction between the iron counter-ion and the Keggin unit in the bulk (a) and in the supported iron-substituted heteropolyacid (b).

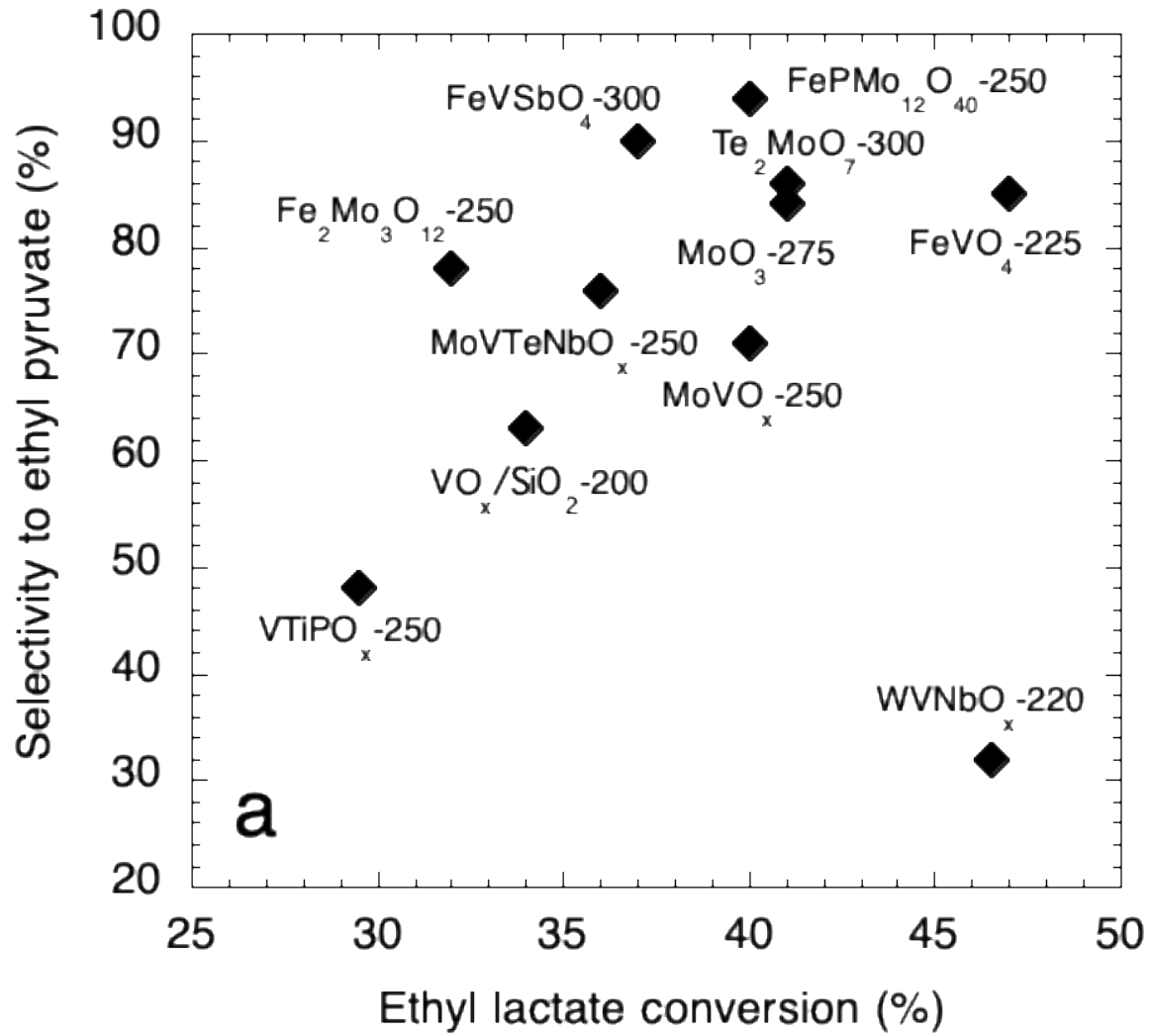
Selectivity to ethyl pyruvate (%)
Ethyl lactate conversion (%)
100
90
80
70
60
50
40
30
20
25
30
35
40
45
50
FeVSbO4-300
FePMo12O40-250
Te2MoO7-300
Fe2Mo3O12-250
MoO3-275
FeVO4-225
MoVTeNbOx-250
MoVOx-250
VOx/SiO2-200
VTiPOx-250
WVNbOx-220
a

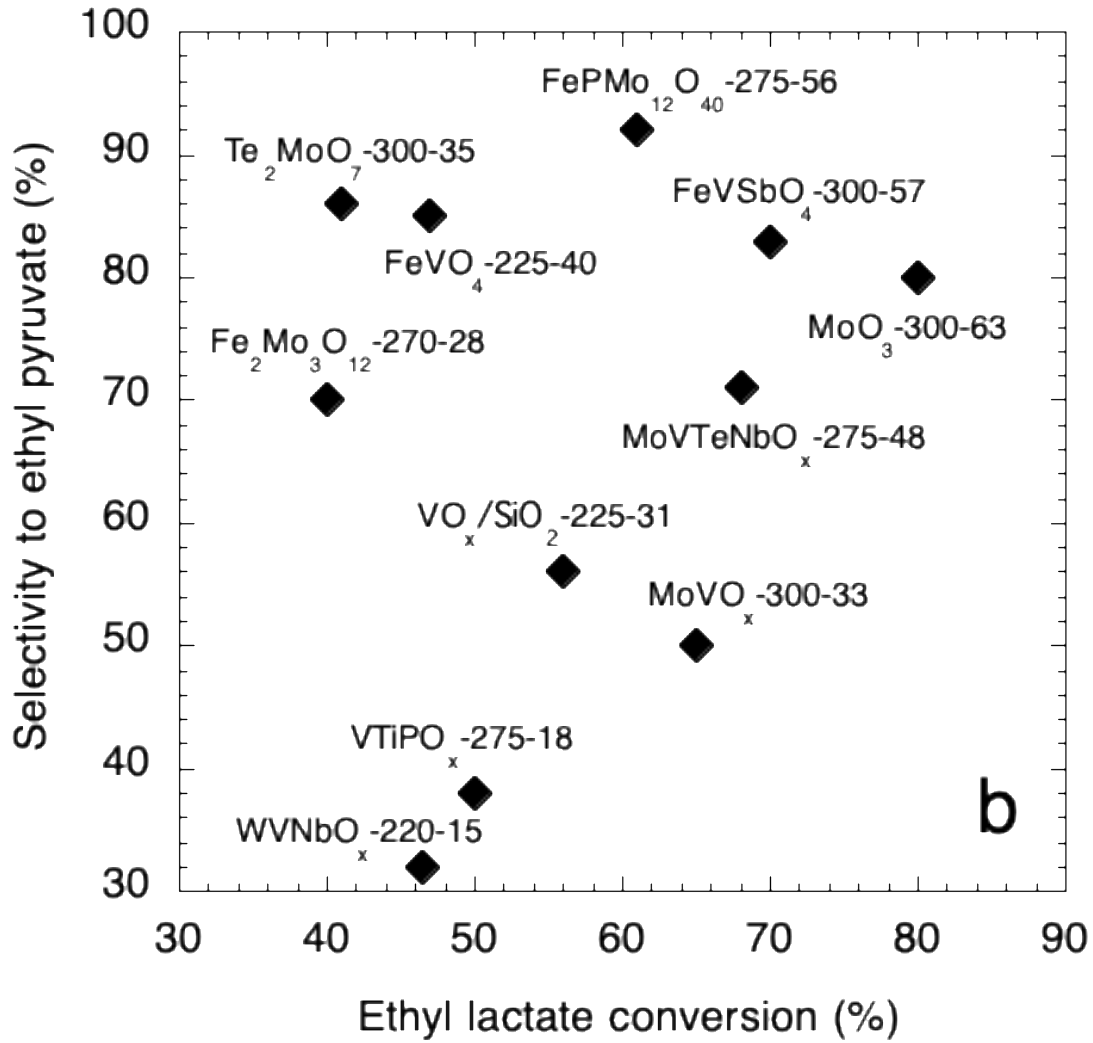
Selectivity to ethyl pyruvate (%)
Ethyl lactate conversion (%)
100
90
80
70
60
50
40
30
30
40
50
60
70
80
90
FePMo12O40-275-56
Te2MoO7-300-35
FeVSbO4-300-57
FeVO4-225-40
MoO3-300-63
Fe2Mo3O12-270-28
MoVTeNbOx-275-48
VOx/SiO2-225-31
MoVOx-300-33
VTiPOx-275-18
WVNbOx-220-15
b

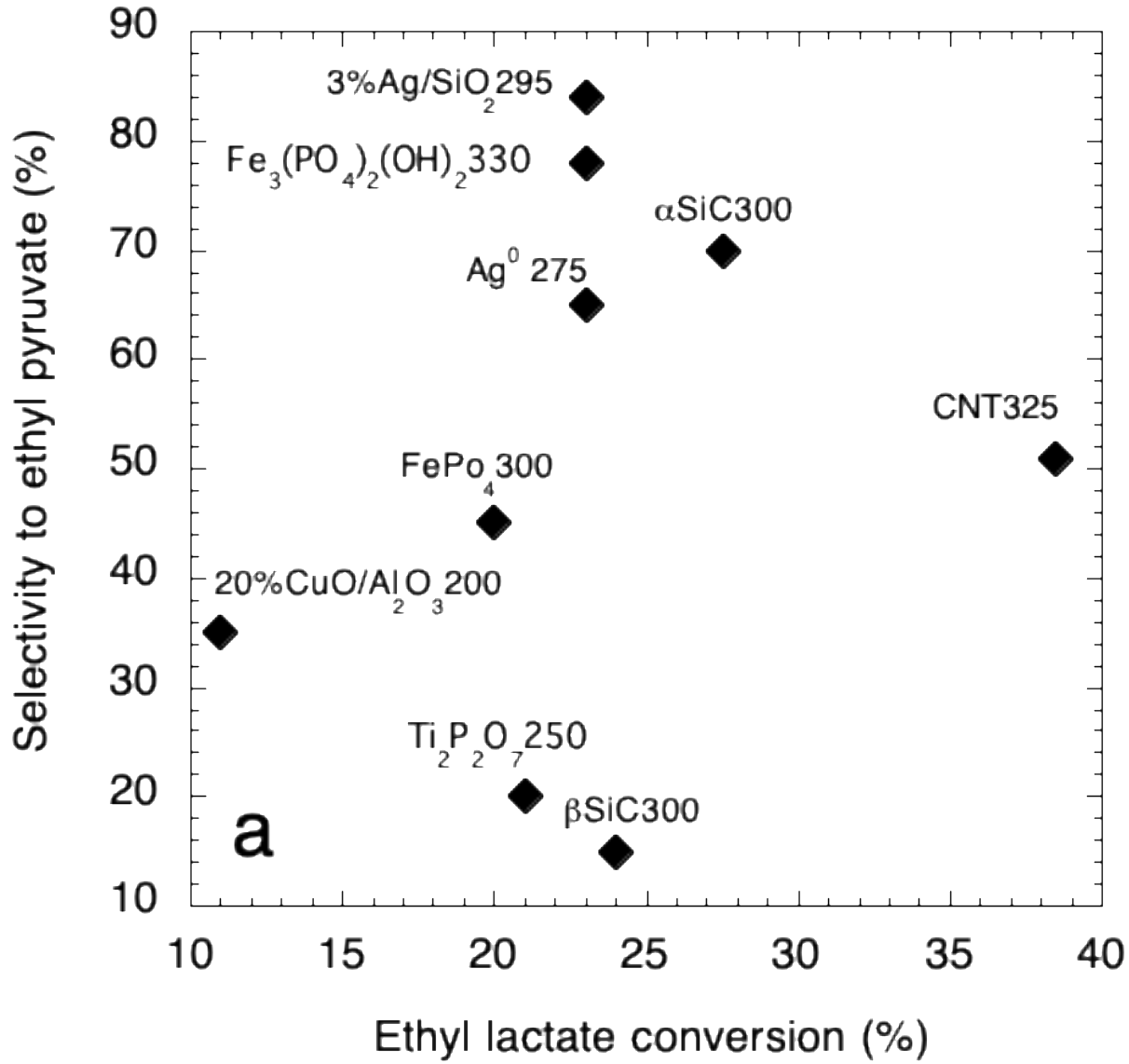
Selectivity to ethyl pyruvate (%)
Ethyl lactate conversion (%)
90
80
70
60
50
40
30
20
10
10
15
20
25
30
35
40
3%Ag/SiO2 295
Fe3(PO4)2(OH)2 330
αSiC300
Ag0 275
CNT325
FePo4 300
20%CuO/Al2O3 200
Ti2P2O7 250
βSiC300
a

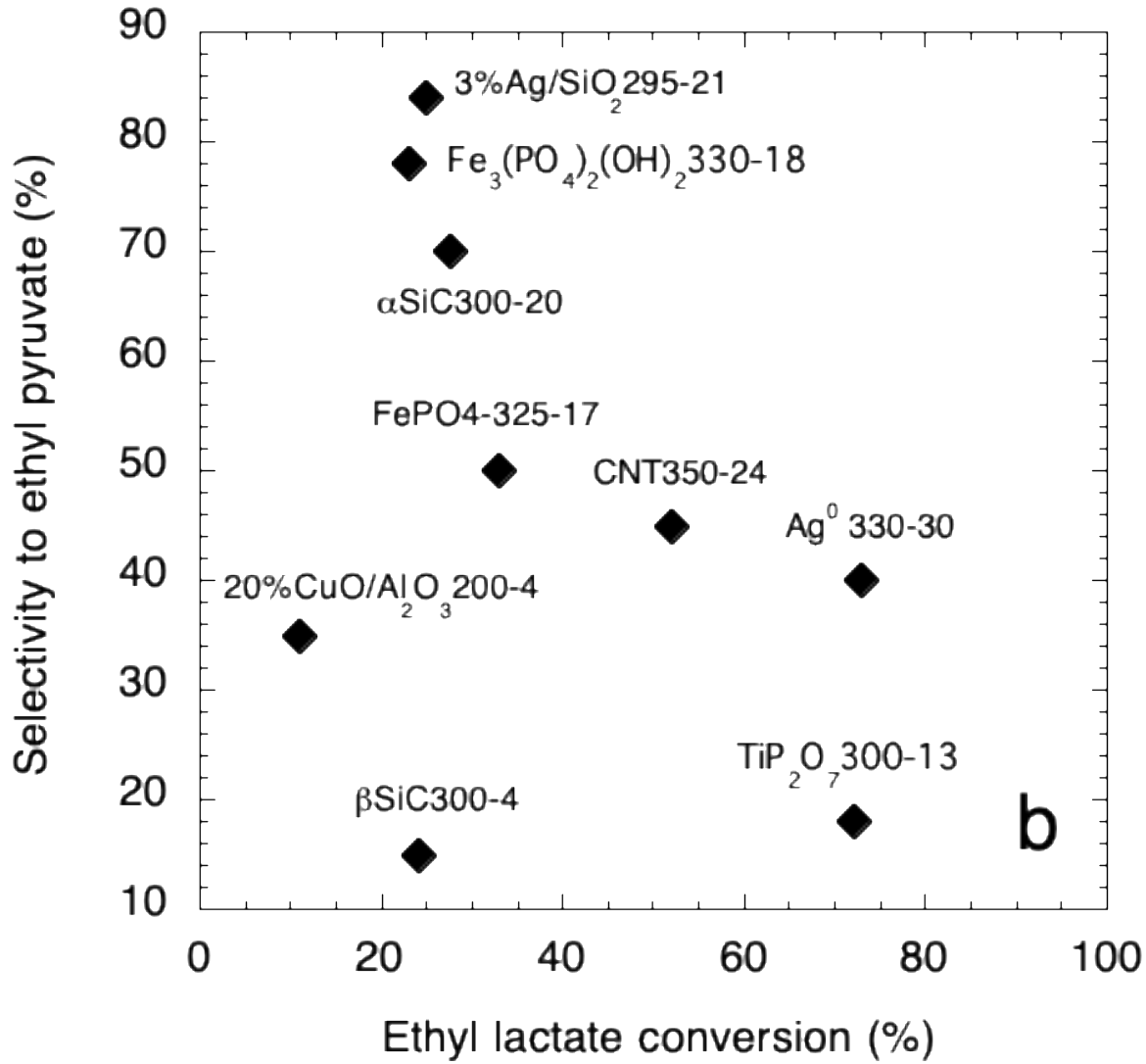
Selectivity to ethyl pyruvate (%)
Ethyl lactate conversion (%)
3%Ag/SiO2 295-21
Fe3(PO4)2(OH)2 330-18
αSiC300-20
FePO4-325-17
CNT350-24
Ag0 330-30
20%CuO/Al2O3 200-4
TiP2O7 300-13
βSiC300-4
b
90
80
70
60
50
40
30
20
10
0
20
40
60
80
100

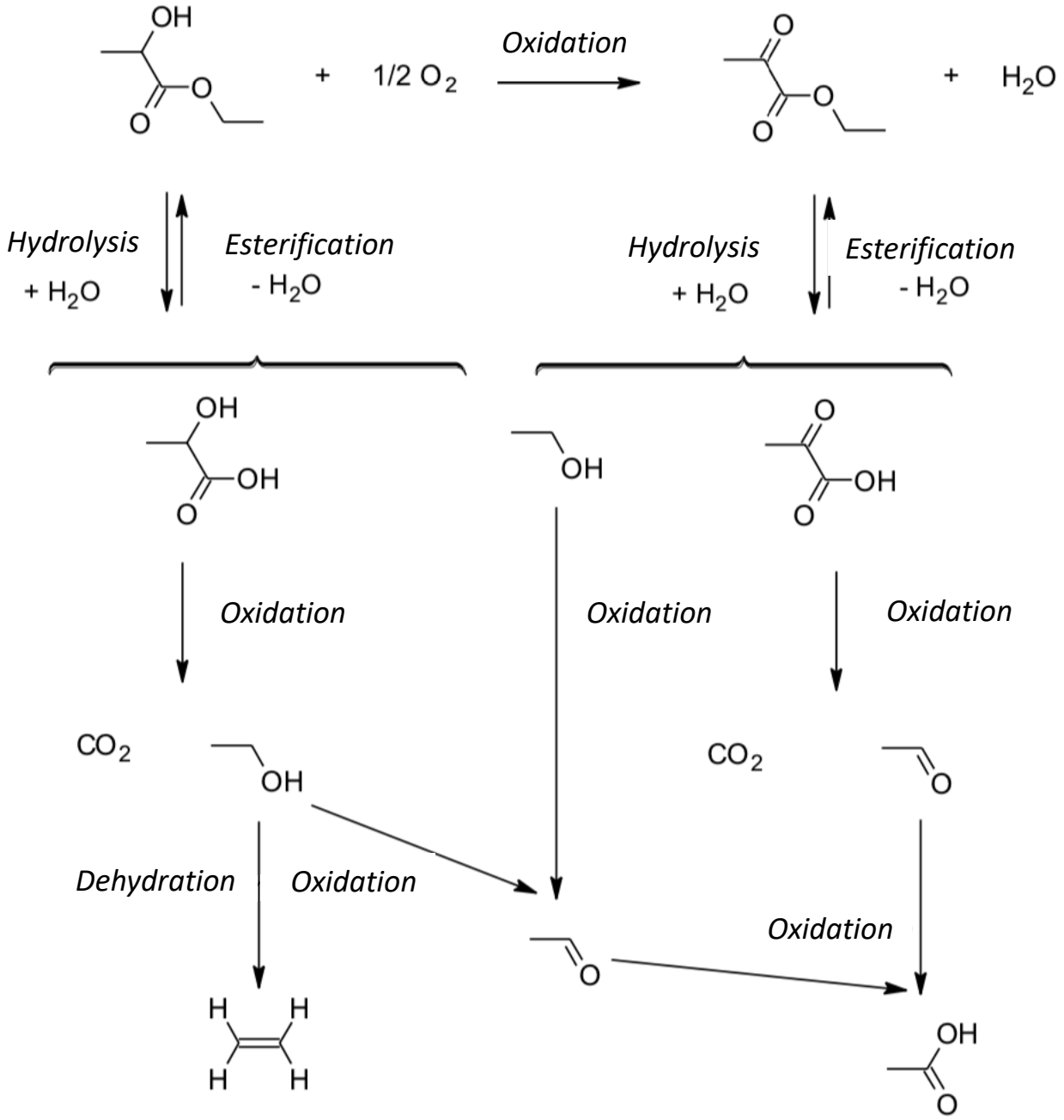
OH
O
O
+ 1/2 O2
Oxidation
O
O
O
+ H2O
Hydrolysis
+ H2O
Esterification
- H2O
Hydrolysis
+ H2O
Esterification
- H2O
OH
OH
O
OH
OH
O
O
OH
Oxidation
Oxidation
Oxidation
CO2
OH
CO2
O
Dehydration
Oxidation
Oxidation
H
H
H
H
O
OH
O

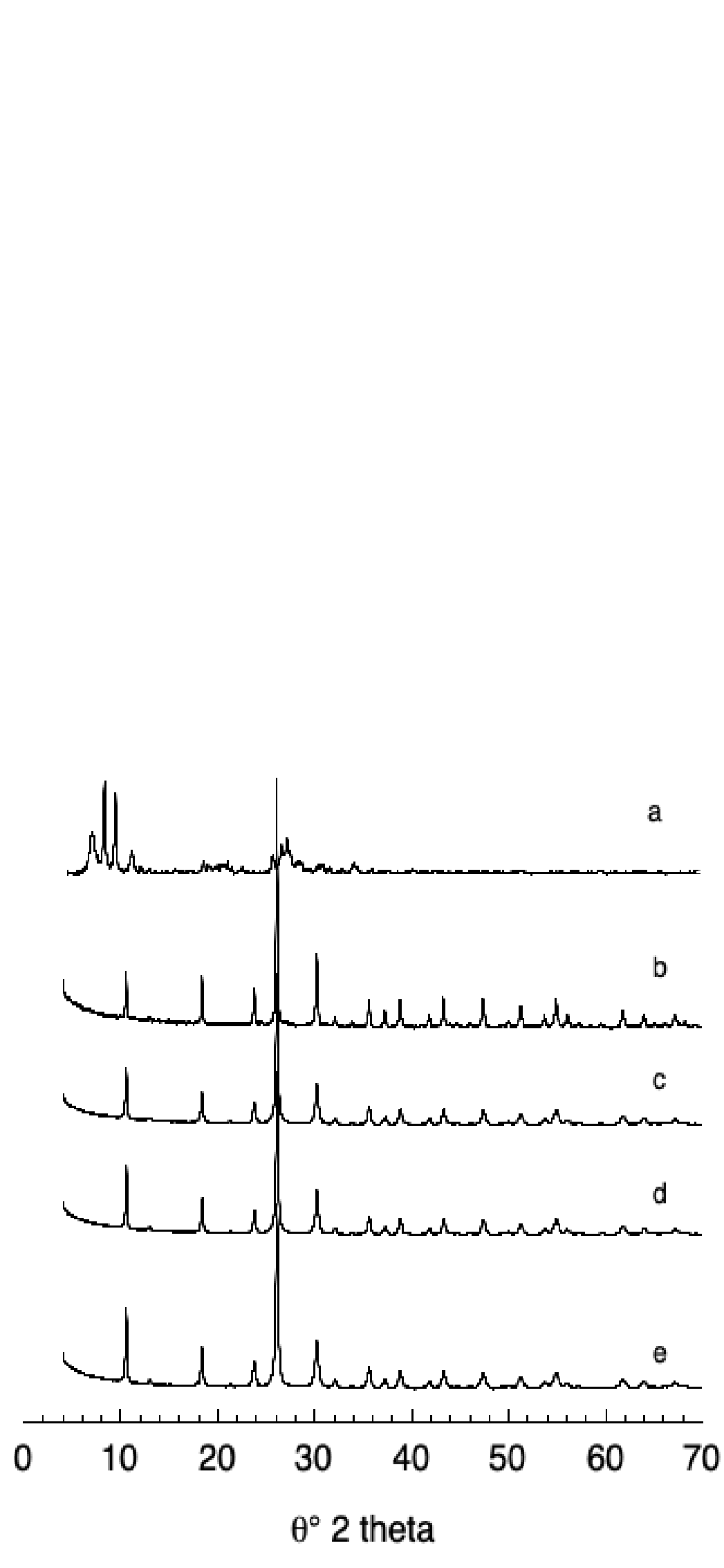
a
b
c
d
e
0
10
20
30
40
50
60
70
θ° 2 theta

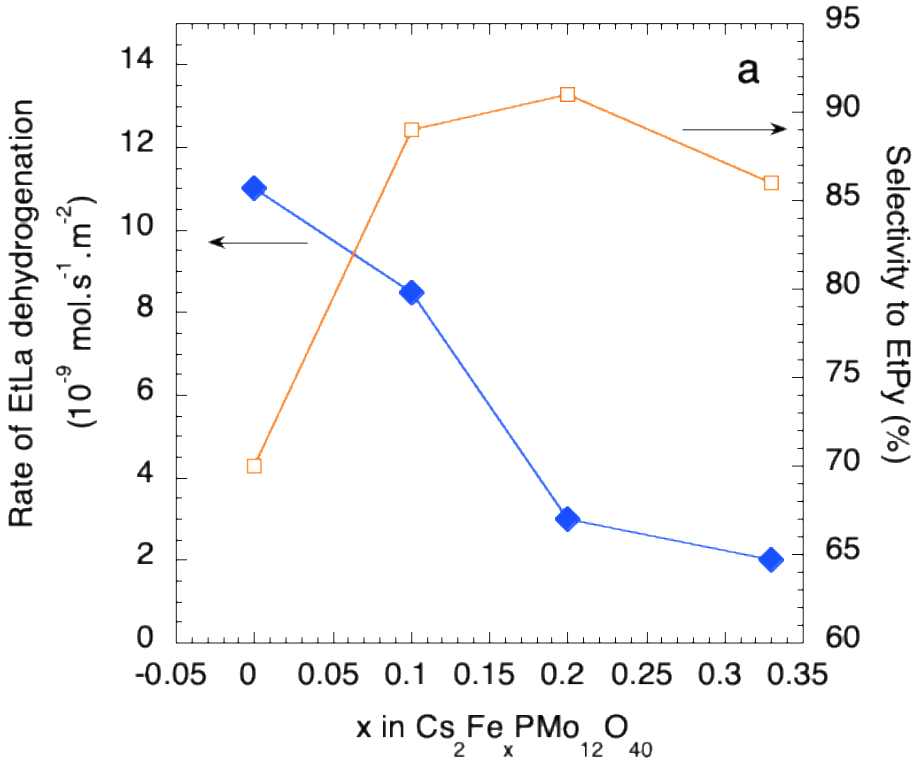
a
Rate of EtLa dehydrogenation
(10^{-9} mol.s^{-1}.m^{-2})
Selectivity to EtPy (%)
x in $Cs_2Fe_xPMo_{12}O_{40}$
0
2
4
6
8
10
12
14
60
65
70
75
80
85
90
95
-0.05
0
0.05
0.1
0.15
0.2
0.25
0.3
0.35

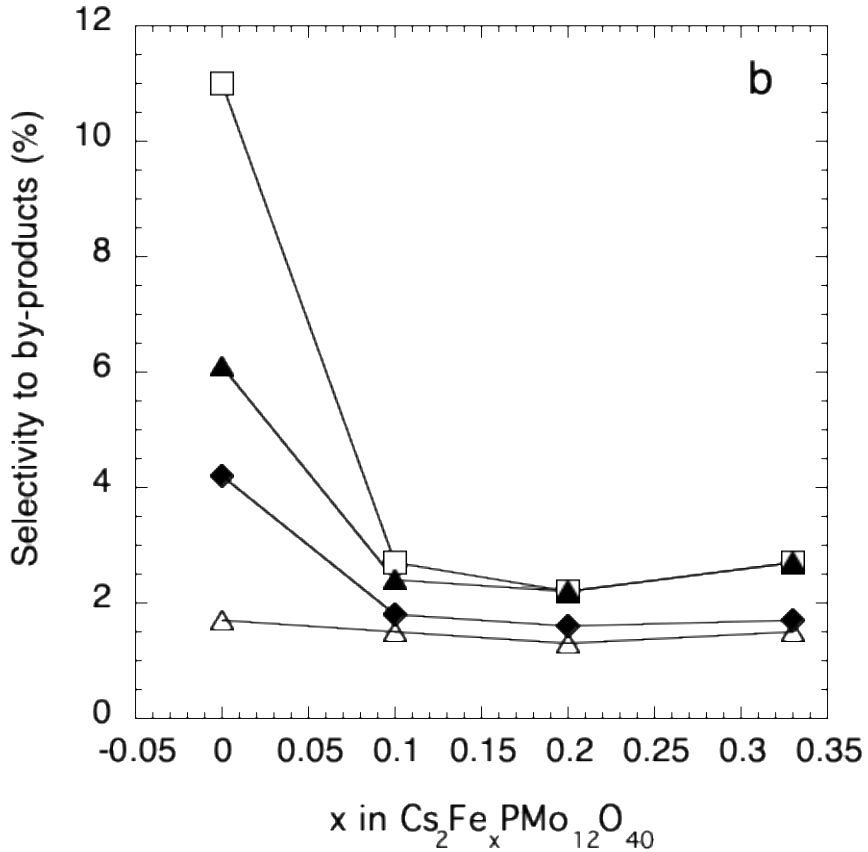
b
Selectivity to by-products (%)
12
10
8
6
4
2
0
-0.05
0
0.05
0.1
0.15
0.2
0.25
0.3
0.35
x in Cs2FexPMo12O40

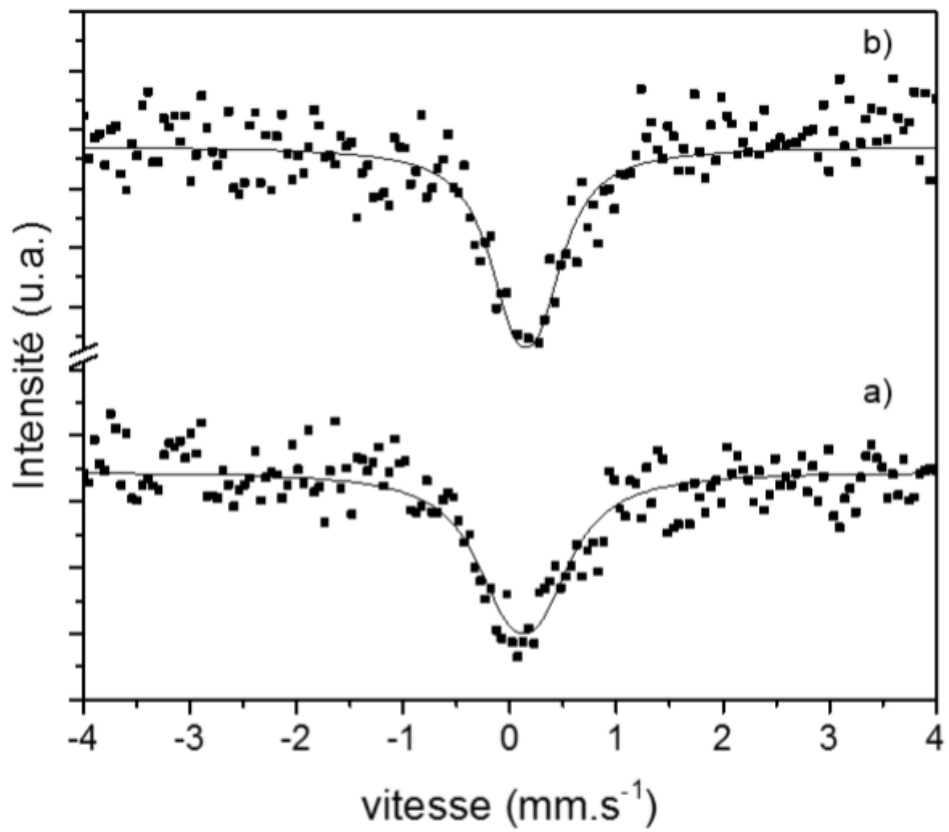
b)
a)
Intensité (u.a.)
-4
-3
-2
-1
0
1
2
3
4
vitesse (mm.s-1)

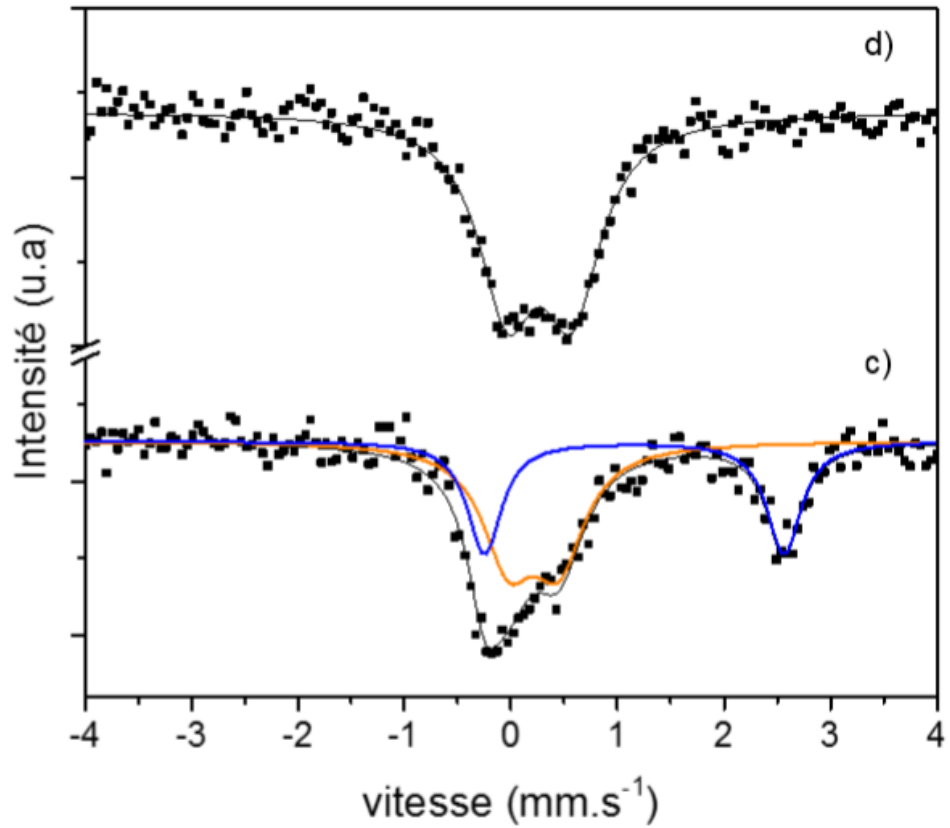
d)
c)
Intensité (u.a)
-4
-3
-2
-1
0
1
2
3
4
vitesse (mm.s-1)

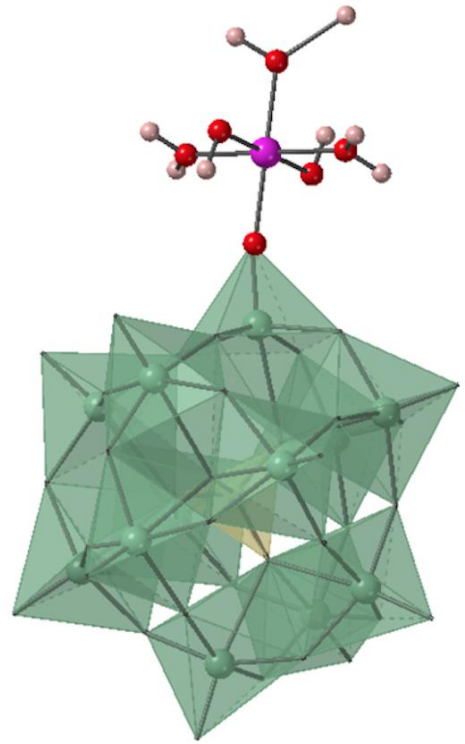

a

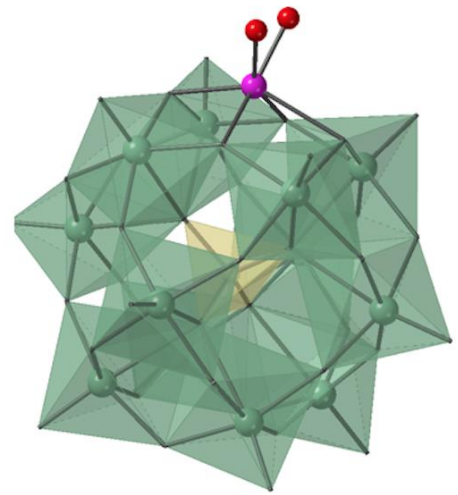

b

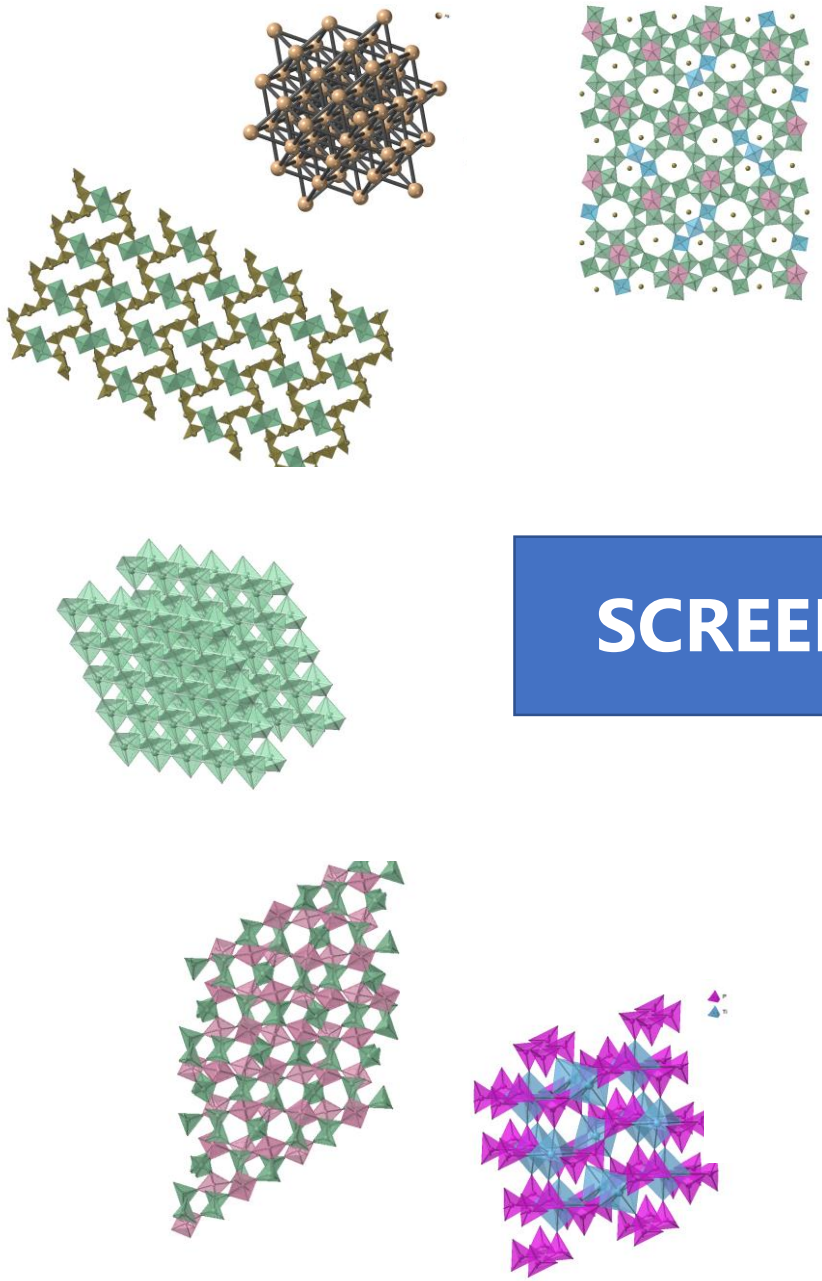

SCREENING

O_2

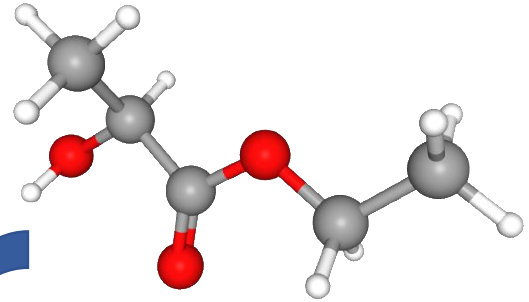

X= 87.1 %

S= 76.8 %

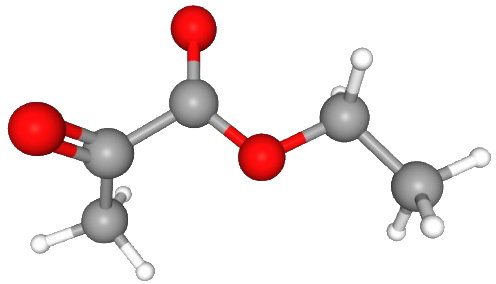

+ H_2O